



OPEN ACCESS

EDITED BY

Xiaoming Jin,
Indiana University–Purdue University
Indianapolis, United States

REVIEWED BY

Jinhui Liu,
Nanjing Medical University, China
Chelsea Hutch,
University of Michigan, United States

*CORRESPONDENCE

Qing Shu
shuqingj@whu.edu.cn

†These authors have contributed
equally to this work and share first
authorship

SPECIALTY SECTION

This article was submitted to
Gut-Brain Axis,
a section of the journal
Frontiers in Neuroscience

RECEIVED 28 April 2022

ACCEPTED 07 July 2022

PUBLISHED 05 August 2022

CITATION

Shao Y, Tian J, Yang Y, Hu Y, Zhu Y and
Shu Q (2022) Identification of key
genes and pathways revealing
the central regulatory mechanism
of brain-derived glucagon-like
peptide-1 on obesity using
bioinformatics analysis.
Front. Neurosci. 16:931161.
doi: 10.3389/fnins.2022.931161

COPYRIGHT

© 2022 Shao, Tian, Yang, Hu, Zhu and
Shu. This is an open-access article
distributed under the terms of the
[Creative Commons Attribution License
\(CC BY\)](https://creativecommons.org/licenses/by/4.0/). The use, distribution or
reproduction in other forums is
permitted, provided the original
author(s) and the copyright owner(s)
are credited and that the original
publication in this journal is cited, in
accordance with accepted academic
practice. No use, distribution or
reproduction is permitted which does
not comply with these terms.

Identification of key genes and pathways revealing the central regulatory mechanism of brain-derived glucagon-like peptide-1 on obesity using bioinformatics analysis

Yuwei Shao^{1†}, Jun Tian^{1†}, Yanan Yang², Yan Hu¹, Ye Zhu³ and Qing Shu^{1*}

¹Department of Rehabilitation, Zhongnan Hospital of Wuhan University, Wuhan, China,

²Department of Traditional Chinese Medicine, China Resources Wugang General Hospital, Wuhan, China, ³College of Health Sciences, Wuhan Sports University, Wuhan, China

Objective: Central glucagon-like peptide-1 (GLP-1) is a target in treating obesity due to its effect on suppressing appetite, but the possible downstream key genes that GLP-1 regulated have not been studied in depth. This study intends to screen out the downstream feeding regulation genes of central GLP-1 neurons through bioinformatics analysis and verify them by chemical genetics, which may provide insights for future research.

Materials and methods: GSE135862 genetic expression profiles were extracted from the Gene Expression Omnibus (GEO) database. The gene ontology (GO) and Kyoto Encyclopedia of Genes and Genomes pathway (KEGG) enrichment analyses were carried out. STRING database and Cytoscape software were used to map the protein-protein interaction (PPI) network of the differentially expressed genes (DEGs). After bioinformatics analysis, we applied chemogenetic methods to modulate the activities of GLP-1 neurons in the nucleus tractus solitarius (NTS) and observed the alterations of screened differential genes and their protein expressions in the hypothalamus under different excitatory conditions of GLP-1 neurons.

Results: A total of 49 DEGs were discovered, including 38 downregulated genes and 11 upregulated genes. The two genes with the highest expression scores were *biglycan* (*Bgn*) and *mitogen-activated protein kinase activated protein kinase 3* (*Mapkapk3*). The results of GO analysis showed that there were 10 molecular functions of differential genes. Differential genes were mainly localized in seven regions around the cells, and enriched in 10 biology processes. The results of the KEGG signaling pathway enrichment analysis showed that differential genes played an important role in seven pathways. The top 15 genes selected according to the Cytoscape software included *Bgn* and *Mapkapk3*. Chemogenetic activation of GLP-1 in NTS induced a decrease in food intake and body mass, while chemogenetic inhibition

induced the opposite effect. The gene and protein expression of GLP-1 were upregulated in NTS when activated by chemogenetics. In addition, the expression of Bgn was upregulated and that of Mapkapk3 was downregulated in the hypothalamus.

Conclusion: Our data showed that GLP-1 could modulate the protein expression of Bgn and Mapkapk3. Our findings elucidated the regulatory network in GLP-1 to obesity and might provide a novel diagnostic and therapeutic target for obesity.

KEYWORDS

glucagon-like peptide-1 (GLP-1), appetite, obesity, bioinformatics, chemical genetics

Introduction

Over the past 40 years, the prevalence of obesity has increased substantially worldwide. The prevalence in children increased from less than 1% in 1975 to 6 to 8% in 2016, in adult males increased from 3 to 11%, and in adult females increased from 6 to 15% during the same period (Jaacks et al., 2019). China has the highest number of obese people in the world, with about 46% of adults and 15% of children suffering from obesity or being overweight (Wang et al., 2019). As one of the most important risk factors for diabetes, cardiovascular disease, cancer, osteoarthritis, movement disorders, and sleep apnea, obesity seriously affects human health (Seidell and Halberstadt, 2015). One of the most effective solutions to obesity is to control appetite and reduce caloric intake (Bray and Siri-Tarino, 2016). Various therapies have shown efficacy to treat obesity, including pharmacotherapy (Narayanaswami and Dwoskin, 2017), operation therapy (Nudel and Sanchez, 2019), and even traditional Chinese medicine (TCM) (Santos et al., 2020; Ni et al., 2021).

Appetite is regulated by a complex system of central and peripheral signals that interact to modulate an individual's response to nutrition. Peripheral regulation

includes satiety signaling and adiposity signaling, whereas central regulation is accomplished by a variety of factors, including the neuropeptidergic, monoaminergic, and endocannabinoid systems. Satiety signals mainly include cholecystokinin (CCK), GLP-1, and casein tyrosine (Valassi et al., 2008).

Glucagon-like peptide 1 is an intestinal hormone that is released in response to food intake. It can enhance the stimulation of insulin synthesis and secretion by glucose while inhibiting the secretion of glucagon and delaying gastric emptying (D'Alessio, 2016). GLP-1 exerts an inhibitory effect on food intake *via* its receptor GLP-1R, which is widely distributed in the brain, gastrointestinal tract, and pancreas (Fakhry et al., 2017). In clinical practice, medication and surgery are widely used. The mechanisms of these interventions in treating obesity are all related to the regulation of GLP-1 (Albaugh et al., 2019; Luo et al., 2020). Some non-pharmaceutical TCM therapies, such as acupuncture, have also shown the potential to affect metabolism by modulating GLP-1 (Firouzjaei et al., 2016). GLP-1 is well-known to medical workers as an important hormone in appetite regulatory pathways, but little is known about how they act in the central nervous system and peripheral nervous system to produce enhanced satiety and inhibit appetite mechanisms. At present, high-throughput gene chip technology and bioinformatics analysis have been widely used in the pathogenesis of diseases, molecular diagnosis, and other aspects (Huang et al., 2018). New scientific and technological methods represented by genomics approaches provide a large amount of research data for mechanistic studies of appetite regulation. Therefore, in this study, we used high-throughput sequencing data from public platforms to decipher the central regulatory mechanism of GLP-1R agonist (GLP1-RA) administration through a bioinformatics approach. Overall, this study advances our understanding of the central mechanisms that synergize the inhibitory effects of appetite and body weight to treat obesity and provides a basis for further research.

Abbreviations: GLP-1, glucagon-like peptide 1; GEO, gene expression omnibus; GO, gene ontology; KEGG, Kyoto encyclopedia of genes and genomes pathway; PPI, protein-protein interaction; DEGs, differentially expressed genes; NTS, nucleus tractus solitarius; Bgn, biglycan; Mapkapk3, mitogen-activated protein kinase activated protein kinase 3; TCM, traditional Chinese medicine; CCK, cholecystokinin; GLP1-RA, GLP-1 receptor agonist; RIP-Seq, RNA co-immunoprecipitation combined with high-throughput sequencing; DVC, dorsal vagal complex; MBH, medial basal hypothalamus; logFC, log value of gene fold change; BP, biological process; MF, molecular function; CC, cellular component; FDR, false discovery rate; MCC, maximal clique centrality; rAAV, adeno-associated virus; cre, cyclization recombination enzyme; CNO, clozapine-N-oxide; WB, Western blotting; RT-qPCR, reverse transcription-quantitative polymerase chain reaction; cDNA, complementary DNA; IF, immunofluorescence; IOD, integrated optical density; AP, posterior area; ECM, extracellular matrix; Erk1/2, extracellular signal-regulated kinase; JNK, c-Jun N-terminal kinase.

Materials and methods

Gene chip data acquisition

The high-throughput dataset GSE135862 related to the mechanisms of appetite regulation by GLP-1/CCK was retrieved and downloaded from GEO, a comprehensive database of gene expression. The chip contains a total of 48 samples. All of the studies were conducted in 9- to 10-week-old C57/Bl6 male mice, which were maintained on standard chow and fasted for 6 h before treatment administration. Multiple variables such as injection of drugs, injection sites, and group settings were included in the experimental conditions. Mice were randomized into treatment groups and received an IP injection of saline, AC710222, exenatide, AC3174, AC170222, or a combination of these drugs twice daily for 5 days. The injection sites were the dorsal vagal complex (DVC) and the medial basal hypothalamus (MBH), respectively. The experimental content is RIP-Seq (RNA co-immunoprecipitation combined with high-throughput sequencing). The purpose of this study was to investigate the pathway of GLP-1 in the brain. In this study, we selected the groups injected with GLP1-RA AC3174 and the blank control group for data comparison and analysis.

Screening of differentially expressed genes

Samples injected with drug as saline were set as the control group and samples injected with drug as GLP1-RA were set as the intervention group using $P < 0.05$, log value of gene fold change (logFC) < -1 , or logFC > 1 as the criterion (Zhang et al., 2019). The GSE135862 dataset was analyzed by the R language DESeq2 package to screen differentially expressed genes between different groups of the dataset and find out differentially expressed genes that may be involved in the regulation of appetite by GLP-1R.

Gene ontology and Kyoto encyclopedia of genes and genomes pathway enrichment analysis of differentially expressed genes

Gene ontology is a commonly used analytical method whose main function is to annotate genes or their products and identify the characteristic biological characteristics of high-throughput genomic or transcriptome data. GO annotates and classifies genes according to Biological Process (BP), Molecular Function (MF), and Cellular Component (CC). The KEGG database is available for querying pathway information and signaling pathway retrieval, and so on. The main goal of

the KEGG database is to endow genes and genomes with functional significance at the molecular level and higher levels, which establish links between genes in the genome and advanced functions of cells and organisms (Kanehisa et al., 2016, 2017). This study used the DAVID (version: 6.8)¹ database for integrative analysis. Using Fisher Exact or EASE Score statistical methods, GO items were screened with $P < 0.05$, false discovery rate (FDR) < 1 , and KEGG items with $P < 0.05$ (Sherman et al., 2007).

Analysis of differentially expressed gene protein interaction network

STRING (version: 11.5)² is an online analysis tool that can be used to present and evaluate interactions between proteins (Szkarczyk et al., 2019). The magnitude of the likelihood of a protein is evaluated by scoring its mutual-action network. In this study, the analyzed differential genes were input into the STRING analysis tool to find potential links between them. The screening condition for constructing the interaction network of differentially gene-encoded proteins was the threshold of interaction likelihood. The STRING database export results were then imported into Cytoscape 3.9.1 software for visual analysis. The cytoHubba plugin in the software was used to find out the top 15 hub genes scored according to the Maximal Clique Centrality (MCC) and Degree scoring methods, respectively (Hu and Chan, 2013).

Preparation of recombinant adeno-associated virus

Promoter sequences of GLP-1 protein were determined by searching the gene database and published relevant literature (Rasouli et al., 2011; Shi et al., 2017). Customized recombinant adeno-associated virus (rAAV), which included GLP-1 promoter and cyclization recombination enzyme (cre) applied in this experiment, was provided by Wuhan BrainVTA Technology Co., Ltd. The sequences of the other three rAAVs are as follows: rAAV-Efla-DIO-EGFP-WPRE-pA (rAAV-GFP), rAAV-hSyn-DIO-hM3D (Gq) -mCherry-WPRE-pA (rAAV-HM3D), and rAAV-hSyn-DIO-hM4D (Gi) -mCherry-WPRE-pA (rAAV-HM4D), which were purchased from commercial companies (BrainVTA Co., Ltd, Wuhan, China).

¹ <https://david.ncifcrf.gov/>

² <https://cn.string-db.org/>

Animals and intervention

We acquired 15 male Sprague–Dawley rats, aged 6 weeks, and weighing 180 to 200 g from Beijing Vital River Laboratory Animal Technology Co., Ltd. (Beijing, China, No. 11400700298971). All rats were placed in a controlled environment at $22 \pm 2^\circ\text{C}$ and $50 \pm 10\%$ relative humidity with a 12-h light/12-h dark cycle in the Experimental Animal Center, Zhongnan Hospital of Wuhan University, with standard food and water provided *ad libitum* for the duration of the study. The study protocol was authorized by the Institutional Animal Care and Use Committee of Wuhan University, Wuhan City, Hubei Province, China (AUP Number: WP2020-08085).

After 1 week of adaptive feeding, all rats were numbered according to body weight, and 15 rats were divided into the GLP-1 group ($n = 5$), HM3D group ($n = 5$), and HM4D group ($n = 5$) by stratified randomization. Stereotactic injection of NTS was performed according to validated parameters (AP: Lambda-3.2 mm, ML: ± 0.5 – 0.7 mm, DV: 9.6 mm, and oblique angle backward 24°) for injection (Shu et al., 2020). Rats in each group were injected with rAAV as follows: rats in the GLP-1 group were injected with rAAV-GLP-1 and rAAV-GFP into NTS with 260 nl of each rAAV; rats in the HM3D group were injected with rAAV-GLP-1 and rAAV-3D into NTS, 260 nl of each rAAV; and rats in HM4D group were injected with rAAV-GLP-1 and rAAV-4D, 260 nl of each rAAV. The chronological order of injection was based on the body weight of the rats, and the rats whose body weight first reached about 400 g were injected first, and finally, the NTS virus injection was completed in all rats at about 5 days. All rats were observed for 1 week after the completion of the injection, with the supplement of food and water *ad libitum* during the observation period. Specific rAAV gene sequence and combinatorial strategy were shown in Figure 1. Three weeks after rAAV injection in all rats, the exogenous gene carried by rAAV was expressed in target neurons. We collected the baseline data of all rats (body mass, Lee's index, and 24 h food intake) 3 weeks after the injection of the last rat, and assigned this day as day 0. Rats in all three groups received four times intraperitoneal injections of Clozapine-N-oxide (CNO) at a dose of 1 mg/kg on the 1st, 3rd, 6th, and 9th day of the experiment (Gomez et al., 2017).

Behavior test

After collecting the baseline data on day 0 of the experiment, we intraperitoneally injected CNO into all rats on the 1st day and recorded the cumulative food intake at 0.5, 1, 2, and 24 h after injection to evaluate the short-term feeding behavior of rats after regulating neuronal excitability. Subsequently, we recorded the cumulative 24 h food intake after the rats received CNO injection and body weight on the 3rd, 6th, and 9th days of the experiment, which aims to observe the long-term

feeding behavior and body weight changes of rats after multiple regulations of neuronal excitability.

Western blotting

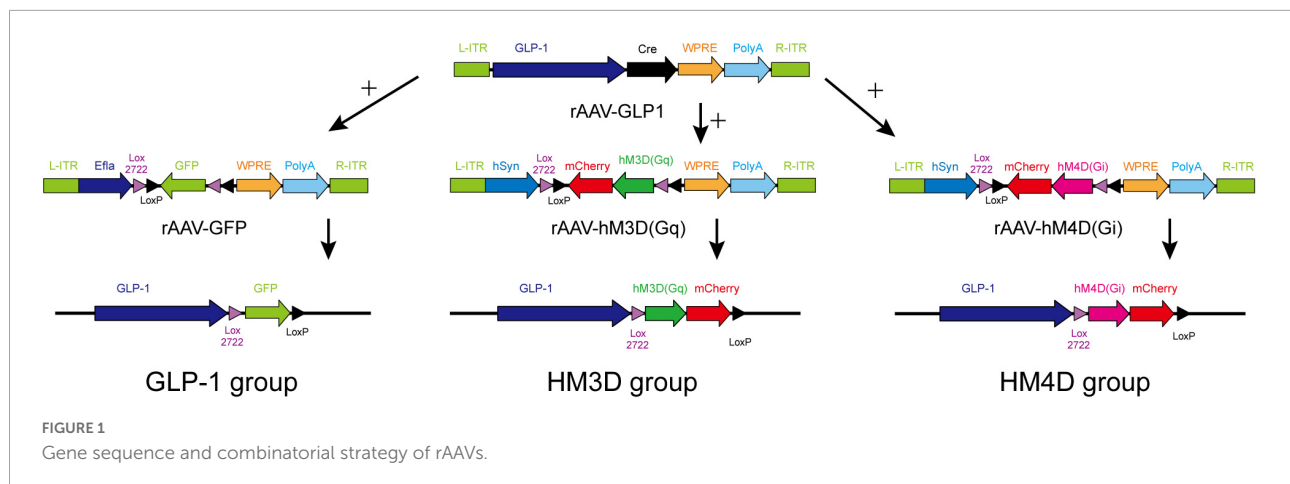
All rats were anesthetized and sacrificed by cervical dislocation after 9 days of treatment. Thirty minutes before sacrifice, rats in HM3D and HM4D groups were in intraperitoneal injection with CNO to activate or inhibit GLP-1 neurons. We froze the tissue of NTS and hypothalamus in liquid nitrogen after stripping them from the rat brains and stored them at -80°C . NTS tissue was detected with GLP-1 antibody, while hypothalamus tissue was detected with Bgn antibody and Mapkapk3 antibody applying a standard WB protocol. The primary antibody concentrations were as follows: GLP-1 (1:1000, AF0166, Affinity, Japan), Bgn (1:1000, 16409-1-AP, Proteintech, China), and Mapkapk3 (1:1000, 15424-1-AP, China). We used the housekeeping protein β -actin (1:1000; Proteintech, China) for normalization. We performed WB in triplicate for all target proteins. Protein expression was calculated based on the target protein and β -actin ratios of optical density, which we analyzed using the BandScan software.

Reverse transcription-quantitative polymerase chain reaction

We isolated total RNA of rat NTS and hypothalamus stored at -80°C with an AZfresh total RNA extraction kit (15596-026, Ambion, United States) and determined RNA concentrations at an absorbance ratio of 260/280 nm. We then reverse transcribed an aliquot (1 μg) of extracted RNA into first-strain complementary DNA (cDNA) using a ReverTra Ace qPCR RT kit (R223-01, VAZYME). We quantified gene expression of GLP-1 of NTS, Bgn, and Mapkapk3 of the hypothalamus by using an SYBR Green real-time PCR Master Mix Plus (Q111-02; VAZYME) and standard protocol. Measurements were conducted in triplicate under standard reaction conditions, and normalization was ensured to β -actin. We obtained primaries from the Biofavor Technology Company (Wuhan, China). All temperature circulation and gene amplification were processed in a CFX96 Touch real-time PCR detection system (Bio-Rad). All RT-PCR assays and primer sequences are shown in Table 1.

Immunofluorescence staining

Rats were anesthetized with isoflurane and received transcardial perfusion with saline and 5% paraformaldehyde. Rat brains were immersion in 5% paraformaldehyde for 72 h for perfusion fixation followed by dehydration in 25% sucrose solution. The coronal plane where the NTS and hypothalamus



are located was selected for the frozen section. The frozen sections in the NTS area with a thickness of 10 μm were selected. After thawing by natural gradient, 10% donkey serum or goat serum was used for blocking. After repairing with sodium citrate antigen retrieval solution, which leads the virus fluorescence to be destroyed, the three groups of brain slices were incubated with c-fos primary antibody. In GLP-1 group, GLP-1 neurons were labeled with anti-GFP (1:2000, ab5450, Abcam, United States) + green fluorescent secondary antibody (1:500, Alexa Fluor[®] 488 Donkey Anti-Goat, ab150129, Abcam, United States), and activated neurons were labeled with anti-cfos (#2250S, Cell Signaling Technology, United States) + red fluorescent secondary antibody (1:500, SA00013-8, CoraLite594 Donkey Anti-Rabbit, Proteintech, China). In HM3D and HM4D groups, GLP-1 neurons were labeled with anti-DsRed (632496, TAKARA, Japan) + red fluorescent secondary antibody (1:800, SA00013-4, CoraLite594 Goat Anti-Rabbit, Proteintech, China) and activated neurons were labeled with anti-cfos (1:2000, ab208942, Abcam, United States) + green fluorescent secondary antibody (1:200, SA00013-1, CoraLite488 Goat Anti-Mouse, Proteintech, China). The co-expression of GLP-1 neurons and cfos in the neuron cells indicated that GLP-1 neurons were activated. The activated GLP-1 neurons in the NTS area of each group were counted and statistically analyzed. The protein expression of differential genes in the hypothalamus of rats in each group was demonstrated by immunofluorescence single labeling. The tissue of the hypothalamus was prepared into frozen slices with a thickness of 20 μm , cubed with anti-Bgn (1:100, 16409-1-AP, Proteintech, China) or anti-Mapkapk3 (1:200, 15424-1-AP, Proteintech, China), and labeled with a green fluorescent (1:500, SA00013-2, CoraLite488 Goat Anti-Rabbit, Proteintech, China). Nuclei were stained with DAPI and observed under a fluorescence microscope. The expression of Bgn and Mapkapk3 in the hypothalamus was analyzed by the imagepro plus 6.0 software with integrated optical density (IOD) for fluorescence intensity analysis.

Statistical analysis

SPSS 25.0 software package was used for statistical analysis. The results were expressed as mean \pm standard deviation ($x \pm s$). One-way analysis of variance was used for comparison between groups within the same time period. If there was an overall difference, multiple comparisons with the Tukey's method were used. Repeated measures analysis of variance was used to compare different time points within the same group, and if there were differences, multiple comparisons with the Tukey's method were used. $P < 0.05$ was considered significant.

Results

Differentially expressed gene analysis results

Based on the screening criteria of $P < 0.05$, $|\log\text{FC}| > 1$, 49 related differentially expressed genes were analyzed in the GSE135862 dataset. Among them, there were 11 upregulated differentially expressed genes and 38 downregulated differentially expressed genes. According to the expression

TABLE 1 Real-time PCR primer sequences.

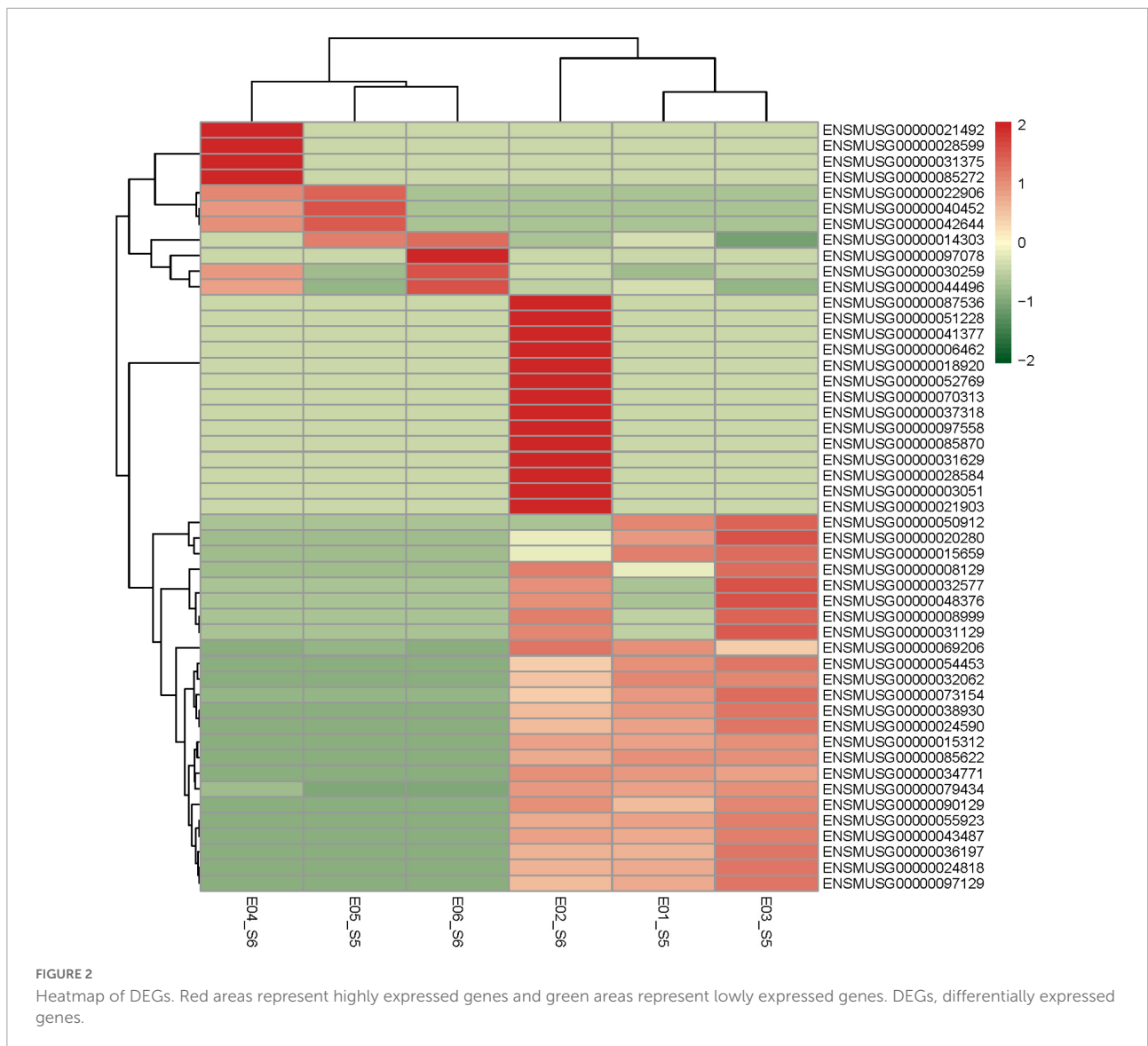
Gene	Primer	Sequence (5'-3')	PCR Products
β -actin	Forward	CACGATGGAGGGGCCGACTCATC	241 bp
	Reverse	TAAAGACCTCTATGCCAACACAGT	
Rat GLP-1	Forward	TCGTGGCTGGATTGTTT	142 bp
	Reverse	TGGCGTTTGTCTTCGTT	
Bgn	Forward	GAGAACAGTGGCTTTGAACC	178 bp
	Reverse	GCTTGGAGTAGCGAAGTAGAT	
Mapkapk3	Forward	GTGCTGGTCTGGGTGTGA	350 bp
	Reverse	CGGTGGCAATGTTCTGG	

fold of the differential genes, the related genes with the largest differential fold were selected, which then upregulated *Bgn* and down-regulated *Mapkapk3*, respectively. A specific heatmap can be seen in Figure 2.

Gene ontology and Kyoto encyclopedia of genes and genomes pathway enrichment analysis results of differentially expressed genes

The results of GO analysis showed that the molecular functions of differential genes mainly included pseudouridine synthase activity, BMP receptor binding, xylosyltransferase activity, proton antiporter activity (sodium, monovalent

cation, potassium), calcium-dependent protein kinase activity, low-density lipoprotein particle receptor activity, transferase activity, and transferring glycosyl and pentosyl groups; differential genes were mainly localized in seven regions around the cells, which were catenin complex, organelle membrane contact site, nuclear outer membrane, varicosity, mitochondria-associated ER membrane, nuclear lamina, and transport vesicle and extracellular matrix; and the biological pathways in which differential genes were involved included apoptotic process involved in development, extracellular structure organization, activation of MAPKK activity, apoptotic process involved in morphogenesis, positive regulation of coagulation, positive regulation of hemostasis, positive regulation of blood coagulation, regulation of apoptotic process involved in development, cell junction maintenance, and regulation of apoptotic process involved in morphogenesis. The results of



KEGG signaling pathway enrichment analysis showed that differential genes played an important role in platelet activation pathway, complement and coagulation cascades pathway, other glycan degradation pathway, other type of O-glycan biosynthesis pathway, cellular senescence pathway, cytokine-cytokine receptor interaction pathway, and apoptosis pathway. Specific results can be seen in **Figure 3**.

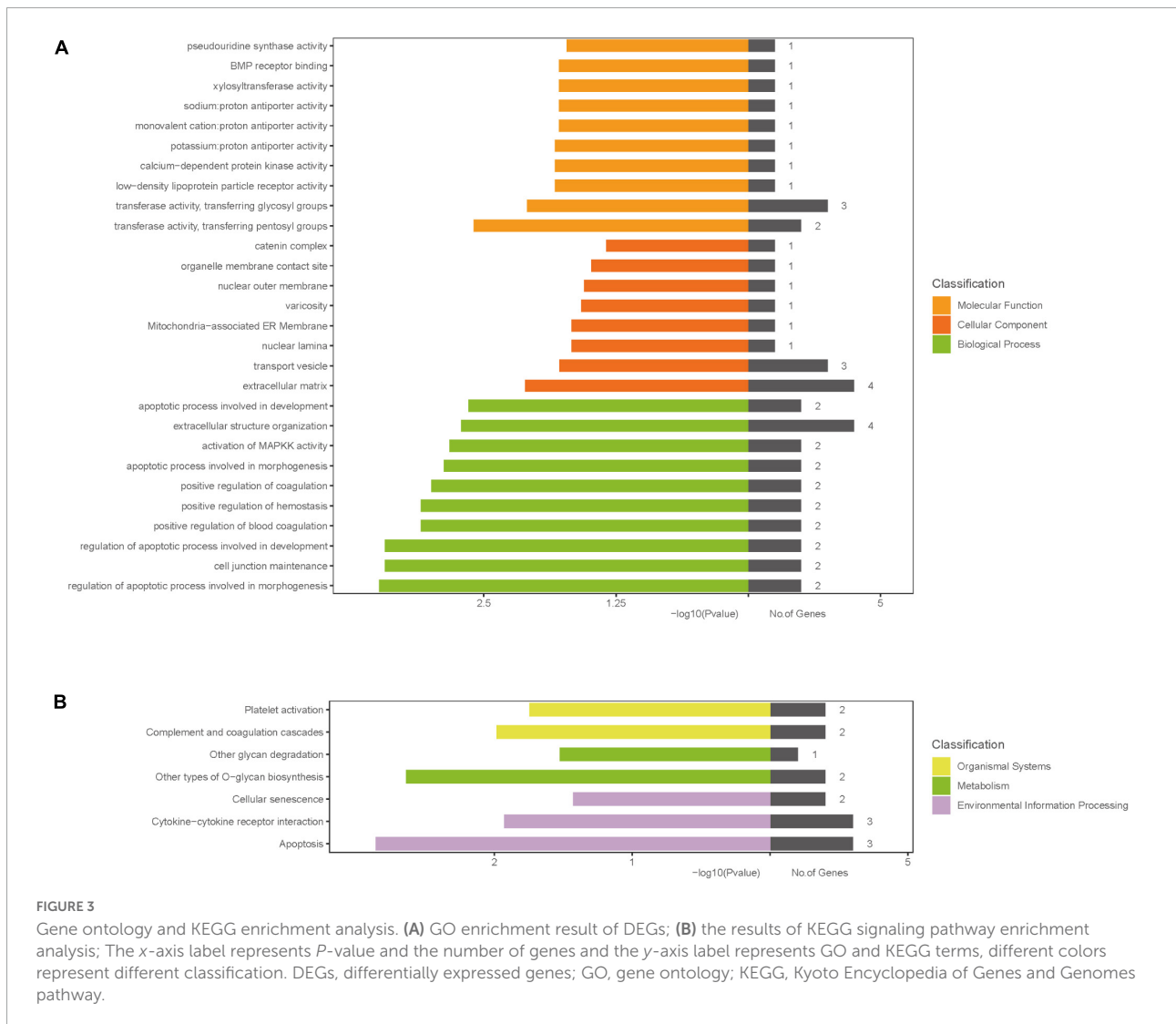
Cytoscape, the key nodes and subnetworks in the PPI network are predicted and explored by several topological algorithms using the cytoHubba plugin. The top 15 genes selected according to the MCC and degree method were *F12*, *Gadd45b*, *Cdh12*, *Nyx*, *Mapkapk3*, *Bgn*, *Tnf*, *Lmnb1*, *Trnfrsf1b*, *F2r*, *Bmpr1a*, *Acvr1*, *Bmp7*, *Nog*, and *F2* (**Figures 4B,C**).

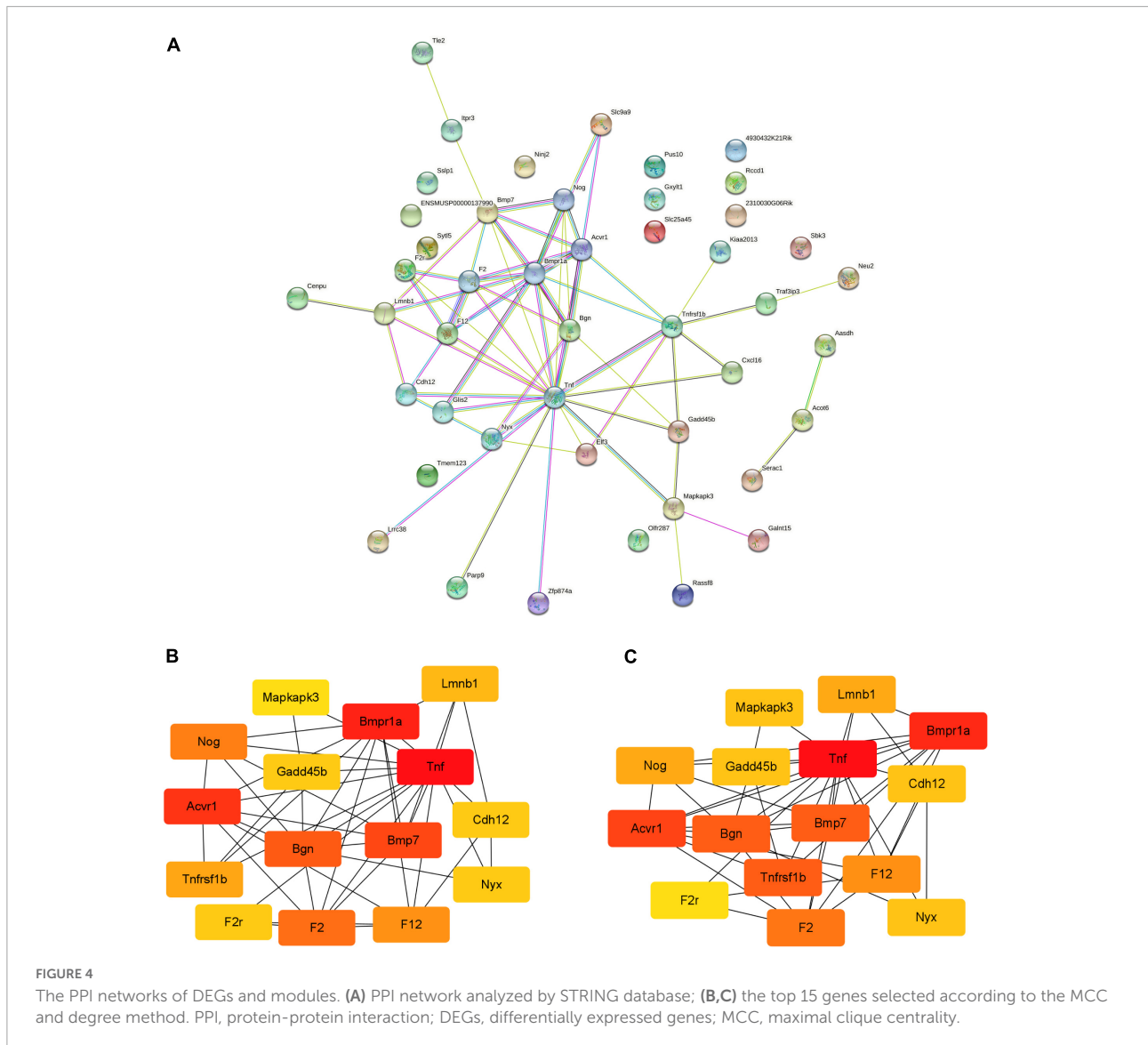
Protein-protein interaction networks and important genes of differentially expressed genes

The PPI network of DEGs and its modules are shown in **Figure 4**. With the STRING database, 46 of 49 DEGs were mapped onto a PPI network. There are 46 nodes and 66 edges (**Figure 4A**). After the PPI network is imported into

Different glucagon-like peptide 1 neuronal excitability modulates appetite-related behavior

As shown in **Figures 5A–C**, there was no significant difference in body weight, Lee’s index, and 24-h food intake among the three groups before intervention ($P > 0.05$). After the first time of CNO injection, the feeding behavior of the three groups of rats showed significant differences (**Figure 5D**).



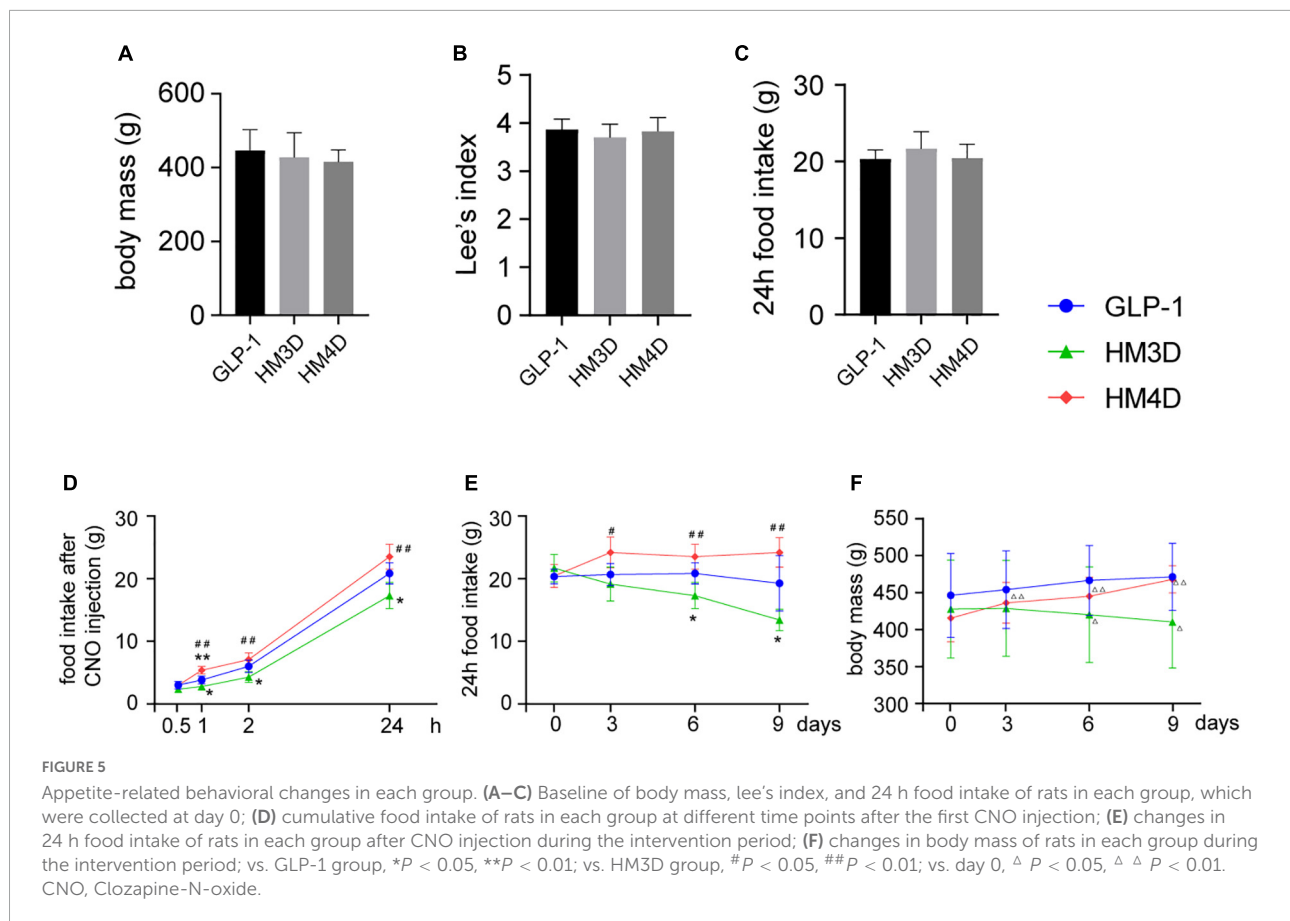


Compared with the GLP-1 group, rats in the HM3D group showed a significant reduction in food intake from 1 h after CNO injection ($P < 0.05$), and the cumulative food intake was significantly lower than that in the GLP-1 group at 1 h, 2 h, and 24 h after CNO injection ($P < 0.05$ or $P < 0.01$). Compared with the GLP-1 group, the HM4D group showed a significant increase in food intake only at 1 h after CNO injection ($P < 0.01$); compared with the HM3D group, the food intake of the HM4D group increased significantly at 1, 2, and 24 h after injection ($P < 0.05$ or $P < 0.01$). There was no statistical difference in the 24-h food intake before CNO injection among the groups of rats, which showed the highest food intake in the HM4D group and the lowest food intake in the HM3D group on days 3, 6, and 9 of injection (Figure 5E). The body weights of rats in the three groups showed different trends during the experiment. Rats in the GLP-1 group did not

show significant variation in body weights after CNO injection. The body weights of rats in the HM3D group were lower than the baseline since the 6th day after CNO injection ($P < 0.05$), and the body weights of rats in the HM4D group increased since the 3rd day after CNO injection. However, we did not observe significant differences in body weight among the three groups of rats at each time point (Figure 5F).

Chemical genetics technology can activate or inhibit glucagon-like peptide 1 neurons in the nucleus tractus solitarius

As shown in Figures 6A,B,C, both the protein and gene expression of GLP-1 in NTS were upregulated in the HM3D



group, while in the HM4D group were downregulated. As shown in **Figures 6D,F**, the GLP-1 neurons in the NTS region of the three groups of rats were successfully labeled with GFP or DsRed primary antibody, and the GLP-1 neurons expressed different amounts of c-fos. The number of activated GLP-1 neurons in the HM3D group was significantly higher than that in the GLP-1 group and the HM4D group ($P < 0.05$); the number of activated neurons in the GLP-1 group was higher than that in the HM4D group ($P < 0.05$) (**Figure 6E**). The results indicated that CNO injection could effectively activate or inhibit GLP-1 neurons in NTS.

Different excitatory properties of glucagon-like peptide 1 neurons regulate the protein and gene expression of biglycan and mitogen-activated protein kinase activated protein kinase 3 in the hypothalamus

As shown in **Figures 7A,B**, the activation of GLP-1 neurons upregulated the gene and protein expression of Bgn in the

hypothalamus ($P < 0.01$); while suppressing it induced the opposite effect ($P < 0.01$). On the contrary, activated GLP-1 neurons can downregulate the gene and protein expression of Mapkapk3 in the hypothalamus ($P < 0.01$), while suppressing GLP-1 can activate Mapkapk3 ($P < 0.01$) (**Figures 7C,D**). Observing the fluorescence images of the hypothalamus, it was found that both Bgn and Mapkapk3 proteins were widely expressed in the hypothalamus without obvious cell specificity (**Figure 7E**). By analyzing the fluorescence intensity, we found that the expression of Bgn increased after activation of GLP-1, while Mapkapk3 decreased (**Figure 7F**), which was consistent with the results of WB and qPCR.

Discussion

Glucagon-like peptide 1, a peptide hormone from the intestinal tract, plays a central role in the coordination of postprandial glucose homeostasis (Gribble and Reimann, 2021). Intake and digestion of carbohydrates, fats, proteins, and bile acids are the main physiological stimuli that promote GLP-1 secretion (Gribble and Reimann, 2019). GLP-1 biosynthesis and release are performed by enteroendocrine cells of the intestine, L cells (Song et al., 2019). L cells are more distributed

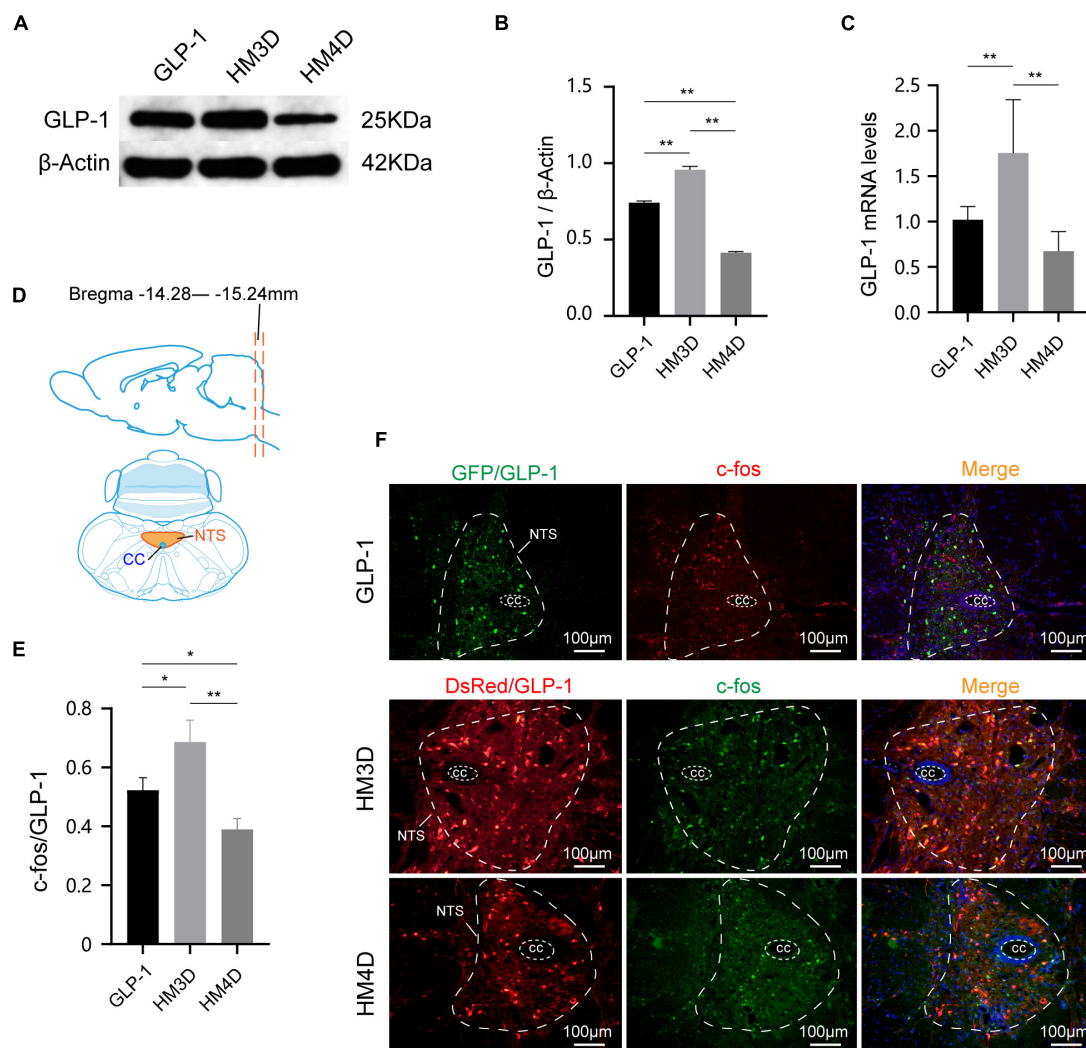


FIGURE 6

Comparison of protein and gene expression of GLP-1 in NTS. (A, B) WB and protein expression of GLP-1 in NTS; (C) gene expression of GLP-1 in NTS; (D) the slice range and localization pattern of the coronal plane where the NTS is located; (E) comparison of activation numbers of GLP-1 neurons in NTS; (F) representative figures of activated GLP-1 neurons in the NTS of rats in each group; * $P < 0.05$, ** $P < 0.01$. WB, Western blotting; GLP-1, glucagon-like peptide 1; cc, central canal; NTS, nucleus of the solitary tract.

in the jejunum, ileum, and colon (Sjolund et al., 1983). Therefore, the stimulation of L cells occurs downstream of food digestion, which is closely related to the local rate of nutrient absorption of the intestine and can control gastric emptying and intestinal tract creeping through feedback regulation (Gribble and Reimann, 2021). Therefore, its main functions include not only stimulating insulin secretion and inhibiting glucagon secretion but also regulating gastrointestinal motility, and working together in many ways to maintain blood glucose homeostasis. In addition to being secreted by the intestine, GLP-1 also exists in neurons of NTS, which release GLP-1 in the central nervous system, including the project to the feeding centers in the hypothalamus (Llewellyn-Smith et al., 2011). GLP-1-mediated neural circuits are the core mechanism by which

GLP-1 neurons in NTS exert their appetite-suppressing effects (Cheng et al., 2020). Therefore, it is also a physiological regulator of appetite and food intake (Holst, 2007).

Glucagon-like peptide 1 exerts its physiological function by binding to a dedicated G-protein-coupled receptor, GLP-1R, expressed in a variety of cell types (Thorens, 1992). Numerous attempts have been made to identify alternative GLP-1R or subtypes, but at present only a single GLP-1R has been identified, whether expressed in the brain, the stomach, or the pancreas (Wei and Mojsov, 1995). In addition to being expressed in the gastrointestinal tract, pancreas, and brain, studies have shown that GLP-1R can be also detected in the vagal afferent nerves, scattered atrial cardiomyocytes, vascular smooth muscle, lung, and some immune cells (Pyke

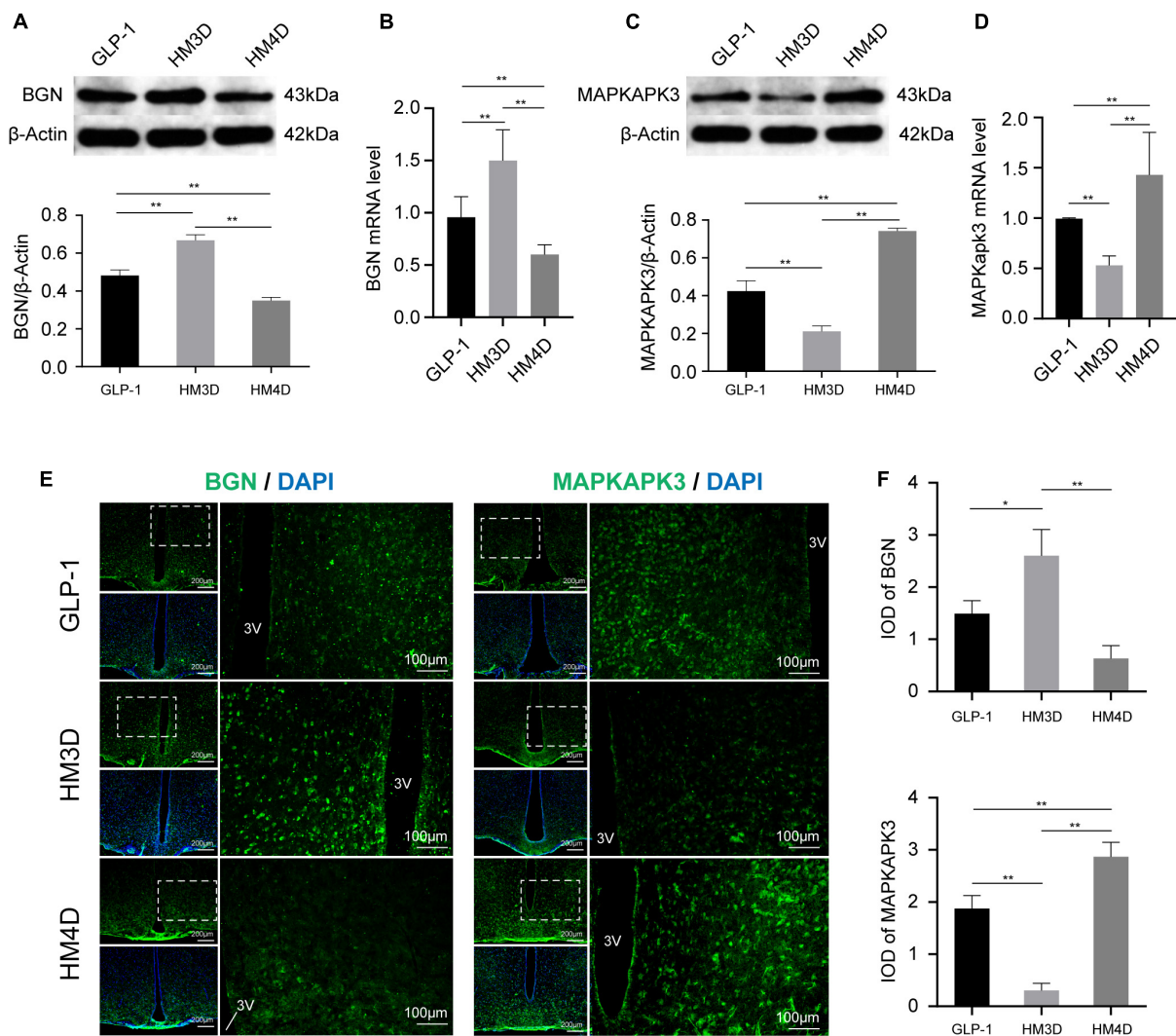


FIGURE 7
 Comparison of protein and gene expression of Bgn and Mapkapk3 in the hypothalamus. (A) WB and protein expression of Bgn in hypothalamus; (B) gene expression of Bgn in hypothalamus; (C) WB and protein expression of Mapkapk3 in hypothalamus; (D) gene expression of Mapkapk3 in hypothalamus; (E) representative figures of Bgn and Mapkapk3 in hypothalamus of rats in each group; (F) comparison of IOD of Bgn and Mapkapk3 in hypothalamus; * $P < 0.05$, ** $P < 0.01$. 3V, the 3rd ventricle. WB, Western blotting; Bgn, biglycan; Mapkapk3, mitogen-activated protein kinase activated protein kinase 3; IOD, integrated optical density.

et al., 2014; Richards et al., 2014; He et al., 2019). The lateral hypothalamic GLP-1R has been identified as an indispensable element of normal food reinforcement, food intake, and body weight regulation (Lopez-Ferreras et al., 2018). As mentioned earlier, GLP-1R-expressing vagal afferent cells have been found to form fibers within the intestinal villi adjacent to enteroendocrine cells. Therefore, it is generally believed that GLP-1R is a chemosensory neuron of the vagal afferents nerve, which helps the vagal afferents nerve receive nutrient detection information in a paracrine manner by binding to GLP-1 released locally by enteroendocrine cells (Krieger et al., 2016; Grill, 2020). Meanwhile, the activity of GLP-1R in vagal afferents also encodes the feeling of distention

in the gastrointestinal tract through the inner ganglia of myenteric plexus intramuscular array detection in gastric and intestinal smooth muscle layers (Williams et al., 2016; Bai et al., 2019). Thus, the vagal afferents of the intestine receive gastrointestinal stimulation through both chemoreceptors and mechanoreceptors to generate neural signals toward the corresponding nuclei of the brainstem, such as those in the NTS and posterior area (AP), then to the hypothalamus, which releases GLP-1 and activates the receptor. However, the current link of this endogenous peripheral GLP-1 indirectly interacting with the central GLP-1 system (via the vagal and/or endocrine pathways) remains controversial, and the necessary intestine-brain circuit has not been empirically confirmed (Brierley

et al., 2021). Therefore, further research in this field should be conducted in the future.

Glucagon-like peptide 1 forms the basis for a variety of current drugs for the treatment of type 2 diabetes and obesity, as well as new agents currently being developed. GLP1-RAs are used clinically to treat T2DM and promote weight loss in people with obesity (Knudsen and Lau, 2019). Although the identity of the GLP1-R-expressing target cells underlying appetite suppression remains under discussion, powerful evidence indicates that GLP1-RAs exert their effects by targeting GLP1-R in the brainstem and/or hypothalamus (Knudsen and Lau, 2019). The mechanism of action of GLP-1 and its receptor in the brain is still unclear, which has caused some difficulties in the optimization of drug development and obesity treatment. Therefore, this study aimed to investigate the differential genes in the brain after GLP1-RAs treatment. After bioinformatics analysis, we found two significantly different genes, *Bgn* of upregulated genes and *Mapkapk3* of downregulated genes.

Biglycan, a class I small leucine-rich proteoglycans, is a key component of the extracellular matrix (ECM) that participates in scaffolding the collagen fibrils and mediates cell signaling. Dysregulation of *Bgn* expression can result in a wide range of clinical conditions such as metabolic disorder, inflammatory disorder, musculoskeletal defects, and malignancies (Appunni et al., 2021). ECM disorganization is a pivotal step in metabolic disorders like obesity which involves accommodating the expanding adipose tissue mass (Kim et al., 2016). The ECM in these states releases non-fibrillar proteoglycans such as *Bgn*, which take part in receptor-mediated interactions to regulate inflammation and organ-specific metabolic disturbances. The ECM plays a role in regulating neurite outgrowth, and neural function and plasticity as well as metabolic diseases (Dityatev et al., 2010). Also, ECM remodeling is crucial for regulating the morphogenesis of the intestine (Bonnans et al., 2014). In this study, GO analysis also found differential genes enriched in ECM. KEGG analysis showed that differential genes play an important role in other types of glycans degradation and biosynthesis pathway. So, the upregulation of *Bgn* expression in this study may indicate increased ECM remodeling, and as previously mentioned, changes in intestinal mechanical signaling can regulate gastrointestinal motility and food intake.

Mitogen-activated protein kinase activated protein kinase 3 is a member of the Mapk signaling pathway family (Wei et al., 2015). The Mapk family is significant in various cellular processes such as apoptosis, oxidative stress, differentiation, inflammatory response, and proliferation, and includes three members: extracellular signal-regulated kinase (Erk1/2), p38, and c-Jun N-terminal kinase (JNK) (Miloso et al., 2008). p38 Mapk is the best-characterized kinase upstream of *Mapkapk3* (Freshney et al., 1994). Studies have shown that p38Mapk can promote β -cell exhaustion in the pancreas, and β -cells can express GLP-1R (Manieri and Sabio, 2015). At the same time, p38 can also regulate the secretion of insulin, and

the insulin level in p38-deficient mice is increased. Then, in this study, *Mapkapk3* is a downstream factor of p38, and the downregulation of *Mapkapk3* may inhibit the p38 Mapk pathway, thereby promoting insulin secretion and increasing the expression of GLP-1R. Studies have shown that the silencing of *Bgn* gene can upregulate p38Mapk (Appunni et al., 2021). In the verification of bioinformatics analysis results, we found that the expression of *Bgn* mRNA was upregulated and the expression of *Mapkapk3* mRNA was downregulated when the GLP-1 neurons were activated, which implied the inhibitory effect of BGN in regulating the p38 pathway from another perspective.

Conclusion

In summary, we screened out the key differential genes that affect feeding behavior after GLP-1R activation through bioinformatics analysis. *Bgn* and *Mapkapk3* were found to be more associated with changes in feeding behavior. Changes in *Bgn* and *Mapkapk3* in the hypothalamus were also detected after activating or inhibiting GLP-1 neurons in the NTS by chemogenetic treatment, which were consistent with the results of bioinformatics analysis. It shows that *Bgn* and *Mapkapk3* may be important downstream cytokines of GLP-1 in regulating appetite, which were worthy of further research in the future.

Data availability statement

The raw data supporting the conclusions of this article will be made available by the authors, without undue reservation.

Ethics statement

The animal study was reviewed and approved by the Institutional Animal Care and Use Committee of Wuhan University.

Author contributions

QS, JT, and YY designed the study protocol and obtained the funding. YS and YH were responsible for the bioinformatics analysis part, animal experimentation, and basic experiment parts. QS was responsible for data analysis. QS, JT, and YS drafted this manuscript. All authors have read and approved the final manuscript, adhere to the trial authorship guidelines, and agreed to publication.

Funding

This work was supported by the Natural Science Foundation of China under grant number (81804180); the Traditional Chinese Medicine Research Project of Hubei Provincial Health Commission (No. ZY2021M031); and the Joint Fund of Hubei Provincial Health Commission under Grant Number (WJ2019H163).

Acknowledgments

We thank all the medical workers in the Department of Rehabilitation Medicine, Zhongnan Hospital of Wuhan University, for their support and assistance in this study.

References

- Albaugh, V. L., Banan, B., Antoun, J., Xiong, Y., Guo, Y., Ping, J., et al. (2019). Role of Bile Acids and GLP-1 in Mediating the Metabolic Improvements of Bariatric Surgery. *Gastroenterology* 104:e1044. doi: 10.1053/j.gastro.2018.11.017
- Appunni, S., Rubens, M., Ramamoorthy, V., Anand, V., Khandelwal, M., and Sharma, A. (2021). Biglycan: an emerging small leucine-rich proteoglycan (SLRP) marker and its clinicopathological significance. *Mol. Cell Biochem.* 476, 3935–3950. doi: 10.1007/s11010-021-04216-z
- Bai, L., Mesgarzadeh, S., Ramesh, K. S., Huey, E. L., Liu, Y., Gray, L. A., et al. (2019). Genetic Identification of Vagal Sensory Neurons That Control Feeding. *Cell* 112:e1123. doi: 10.1016/j.cell.2019.10.031
- Bonnans, C., Chou, J., and Werb, Z. (2014). Remodelling the extracellular matrix in development and disease. *Nat. Rev. Mol. Cell Biol.* 15, 786–801. doi: 10.1038/nrm3904
- Bray, G. A., and Siri-Tarino, P. W. (2016). The Role of Macronutrient Content in the Diet for Weight Management. *Endocrinol. Metab. Clin. North Am.* 45, 581–604. doi: 10.1016/j.eccl.2016.04.009
- Brierley, D. I., Holt, M. K., Singh, A., de Araujo, A., McDougle, M., Vergara, M., et al. (2021). Central and peripheral GLP-1 systems independently suppress eating. *Nat. Metab.* 3, 258–273. doi: 10.1038/s42255-021-00344-4
- Cheng, W., Ndoka, E., Hutch, C., Roelofs, K., MacKinnon, A., Khoury, B., et al. (2020). Leptin receptor-expressing nucleus tractus solitarius neurons suppress food intake independently of GLP1 in mice. *JCI Insight* 5:e134359. doi: 10.1172/jci.insight.134359
- D'Alessio, D. (2016). Is GLP-1 a hormone: whether and When? *J. Diabetes Investig.* 7, 50–55. doi: 10.1111/jdi.12466
- Dityatev, A., Schachner, M., and Sonderegger, P. (2010). The dual role of the extracellular matrix in synaptic plasticity and homeostasis. *Nat. Rev. Neurosci.* 11, 735–746. doi: 10.1038/nrn2898
- Fakhry, J., Wang, J., Martins, P., Fothergill, L. J., Hunne, B., Prieur, P., et al. (2017). Distribution and characterisation of CCK containing enteroendocrine cells of the mouse small and large intestine. *Cell Tissue Res.* 369, 245–253. doi: 10.1007/s00441-017-2612-1
- Firouzaei, A., Li, G. C., Wang, N., Liu, W. X., and Zhu, B. M. (2016). Comparative evaluation of the therapeutic effect of metformin monotherapy with metformin and acupuncture combined therapy on weight loss and insulin sensitivity in diabetic patients. *Nutr Diabetes* 6, e209. doi: 10.1038/nutd.2016.16
- Freshney, N. W., Rawlinson, L., Guesdon, F., Jones, E., Cowley, S., Hsuan, J., et al. (1994). Interleukin-1 activates a novel protein kinase cascade that results in the phosphorylation of Hsp27. *Cell* 78, 1039–1049. doi: 10.1016/0092-8674(94)90278-x
- Gomez, J. L., Bonaventura, J., Lesniak, W., Mathews, W. B., Sysa-Shah, P., Rodriguez, L. A., et al. (2017). Chemogenetics revealed: dREADD occupancy and activation via converted clozapine. *Science* 357, 503–507. doi: 10.1126/science.aan2475
- Gribble, F. M., and Reimann, F. (2019). Function and mechanisms of enteroendocrine cells and gut hormones in metabolism. *Nat. Rev. Endocrinol.* 15, 226–237. doi: 10.1038/s41574-019-0168-8
- Gribble, F. M., and Reimann, F. (2021). Metabolic Messengers: glucagon-like peptide 1. *Nat. Metab.* 3, 142–148. doi: 10.1038/s42255-020-00327-x
- Grill, H. J. (2020). A Role for GLP-1 in Treating Hyperphagia and Obesity. *Endocrinology* 161:bqaa093. doi: 10.1210/endo/bqaa093
- He, S., Kahles, F., Rattik, S., Nairz, M., McAlpine, C. S., Anzai, A., et al. (2019). Gut intraepithelial T cells calibrate metabolism and accelerate cardiovascular disease. *Nature* 566, 115–119. doi: 10.1038/s41586-018-0849-9
- Holst, J. J. (2007). The physiology of glucagon-like peptide 1. *Physiol. Rev.* 87, 1409–1439. doi: 10.1152/physrev.00034.2006
- Hu, A. L., and Chan, K. C. (2013). Utilizing both topological and attribute information for protein complex identification in PPI networks. *IEEE/ACM Trans. Comput. Biol. Bioinform.* 10, 780–792. doi: 10.1109/TCBB.2013.37
- Huang, X., Liu, S., Wu, L., Jiang, M., and Hou, Y. (2018). High Throughput Single Cell RNA Sequencing. *Bioinform. Anal. Appl. Adv. Exp. Med. Biol.* 1068, 33–43. doi: 10.1007/978-981-13-0502-3_4
- Jaacks, L. M., Vandevijvere, S., Pan, A., McGowan, C. J., Wallace, C., Imamura, F., et al. (2019). The obesity transition: stages of the global epidemic. *Lancet Diabetes Endocrinol.* 7, 231–240. doi: 10.1016/S2213-8587(19)30026-9
- Kanehisa, M., Furumichi, M., Tanabe, M., Sato, Y., and Morishima, K. (2017). KEGG: new perspectives on genomes, pathways, diseases and drugs. *Nucleic Acids Res.* 45, D353–D361. doi: 10.1093/nar/gkw1092
- Kanehisa, M., Sato, Y., Kawashima, M., Furumichi, M., and Tanabe, M. (2016). KEGG as a reference resource for gene and protein annotation. *Nucleic Acids Res.* 44, D457–D462. doi: 10.1093/nar/gkv1070
- Kim, J., Lee, S. K., Shin, J. M., Jeoun, U. W., Jang, Y. J., Park, H. S., et al. (2016). Enhanced biglycan gene expression in the adipose tissues of obese women and its association with obesity-related genes and metabolic parameters. *Sci. Rep.* 6:30609. doi: 10.1038/srep30609
- Knudsen, L. B., and Lau, J. (2019). The Discovery and Development of Liraglutide and Semaglutide. *Front. Endocrinol.* 10:155. doi: 10.3389/fendo.2019.00155
- Krieger, J. P., Arnold, M., Pettersen, K. G., Lossel, P., Langhans, W., and Lee, S. J. (2016). Knockdown of GLP-1 Receptors in Vagal Afferents Affects Normal Food Intake and Glycemia. *Diabetes* 65, 34–43. doi: 10.2337/db15-0973
- Llewellyn-Smith, I. J., Reimann, F., Gribble, F. M., and Trapp, S. (2011). Preproglucagon neurons project widely to autonomic control areas in the mouse brain. *Neuroscience* 180, 111–121. doi: 10.1016/j.neuroscience.2011.02.023
- Lopez-Ferreras, L., Richard, J. E., Noble, E. E., Eerola, K., Anderberg, R. H., Olandersson, K., et al. (2018). Lateral hypothalamic GLP-1 receptors are critical

Conflict of interest

The authors declare that the research was conducted in the absence of any commercial or financial relationships that could be construed as a potential conflict of interest.

Publisher's note

All claims expressed in this article are solely those of the authors and do not necessarily represent those of their affiliated organizations, or those of the publisher, the editors and the reviewers. Any product that may be evaluated in this article, or claim that may be made by its manufacturer, is not guaranteed or endorsed by the publisher.

- for the control of food reinforcement, ingestive behavior and body weight. *Mol. Psychiatr.* 23, 1157–1168. doi: 10.1038/mp.2017.187
- Luo, S., Gill, H., Feltis, B., Hung, A., Nguyen, L. T., and Lenon, G. B. (2020). The Effects of a Weight-Loss Herbal Formula RCM-107 and Its Eight Individual Ingredients on Glucagon-Like Peptide-1 Secretion—An In Vitro and In Silico Study. *Int. J. Mol. Sci.* 21:2854. doi: 10.3390/ijms21082854
- Manieri, E., and Sabio, G. (2015). Stress kinases in the modulation of metabolism and energy balance. *J. Mol. Endocrinol.* 55, R11–R22. doi: 10.1530/JME-15-0146
- Miloso, M., Scuteri, A., Foudah, D., and Tredici, G. (2008). MAPKs as mediators of cell fate determination: an approach to neurodegenerative diseases. *Curr. Med. Chem.* 15, 538–548. doi: 10.2174/092986708783769731
- Narayanaswami, V., and Dvoskin, L. P. (2017). Obesity: current and potential pharmacotherapeutics and targets. *Pharmacol. Ther.* 170, 116–147. doi: 10.1016/j.pharmthera.2016.10.015
- Ni, W., Wang, P., Chen, H., Liu, Y., Zhang, W., Qiu, L., et al. (2021). Obesity complicated with insulin resistance treated with the electroacupuncture at the combination of back-shu and front-mu points. *World J. Acupunct.* 32, 213–217.
- Nudel, J., and Sanchez, V. M. (2019). Surgical management of obesity. *Metabolism* 92, 206–216. doi: 10.1016/j.metabol.2018.12.002
- Pyke, C., Heller, R. S., Kirk, R. K., Orskov, C., Reedtz-Runge, S., Kaastrup, P., et al. (2014). GLP-1 receptor localization in monkey and human tissue: novel distribution revealed with extensively validated monoclonal antibody. *Endocrinology* 155, 1280–1290. doi: 10.1210/en.2013-1934
- Rasouli, M., Ahmad, Z., Omar, A. R., and Allaudin, Z. N. (2011). Engineering an L-cell line that expresses insulin under the control of the glucagon-like peptide-1 promoter for diabetes treatment. *BMC Biotechnol.* 11:99. doi: 10.1186/1472-6750-11-99
- Richards, P., Parker, H. E., Adriaenssens, A. E., Hodgson, J. M., Cork, S. C., Trapp, S., et al. (2014). Identification and characterization of GLP-1 receptor-expressing cells using a new transgenic mouse model. *Diabetes* 63, 1224–1233. doi: 10.2337/db13-1440
- Santos, R. V., Rodrigues, J. M., and Jesus, M. I. (2020). Review on the effects obesity treatment with acupuncture and phytoacupuncture. *World J. Acupunct. Moxibustion* 30, 223–228.
- Seidell, J. C., and Halberstadt, J. (2015). The global burden of obesity and the challenges of prevention. *Ann. Nutr. Metab.* 66(Suppl. 2), 7–12. doi: 10.1159/000375143
- Sherman, B. T., Huang, da, W., Tan, Q., Guo, Y., Bour, S., et al. (2007). DAVID Knowledgebase: a gene-centered database integrating heterogeneous gene annotation resources to facilitate high-throughput gene functional analysis. *BMC Bioinform.* 8:426. doi: 10.1186/1471-2105-8-426
- Shi, X., Chacko, S., Li, F., Li, D., Burrin, D., Chan, L., et al. (2017). Acute activation of GLP-1-expressing neurons promotes glucose homeostasis and insulin sensitivity. *Mol. Metab.* 6, 1350–1359. doi: 10.1016/j.molmet.2017.08.009
- Shu, Q., Shao, Y., Tian, J., and Yang, Y. (2020). Preliminary investigation of localization of solitary nucleus microinjection in rats. *Acta Lab. Anim. Sci. Sin.* 28, 429–435.
- Sjolund, K., Sanden, G., Hakanson, R., and Sundler, F. (1983). Endocrine cells in human intestine: an immunocytochemical study. *Gastroenterology* 85, 1120–1130.
- Song, Y., Koehler, J. A., Baggio, L. L., Powers, A. C., Sandoval, D. A., and Drucker, D. J. (2019). Gut-Proglucagon-Derived Peptides Are Essential for Regulating Glucose Homeostasis in Mice. *Cell Metab* 97:e973. doi: 10.1016/j.cmet.2019.08.009
- Szklarczyk, D., Gable, A. L., Lyon, D., Junge, A., Wyder, S., Huerta-Cepas, J., et al. (2019). STRING v11: protein-protein association networks with increased coverage, supporting functional discovery in genome-wide experimental datasets. *Nucleic Acids Res.* 47, D607–D613. doi: 10.1093/nar/gky1131
- Thorens, B. (1992). Expression cloning of the pancreatic beta cell receptor for the gluco-incretin hormone glucagon-like peptide 1. *Proc. Natl. Acad. Sci. U.S.A.* 89, 8641–8645. doi: 10.1073/pnas.89.18.8641
- Valassi, E., Scacchi, M., and Cavagnini, F. (2008). Neuroendocrine control of food intake. *Nutr. Metab. Cardiovasc. Dis.* 18, 158–168. doi: 10.1016/j.numecd.2007.06.004
- Wang, Y., Xue, H., Sun, M., Zhu, X., Zhao, L., and Yang, Y. (2019). Prevention and control of obesity in China. *Lancet Glob. Health* 7:e1166–e1167. doi: 10.1016/S2214-109X(19)30276-1
- Wei, Y., An, Z., Zou, Z., Sumpter, R., Su, M., Zang, X., et al. (2015). The stress-responsive kinases MAPKAPK2/MAPKAPK3 activate starvation-induced autophagy through Beclin 1 phosphorylation. *Elife* 4:e05289. doi: 10.7554/eLife.05289
- Wei, Y., and Mojsov, S. (1995). Tissue-specific expression of the human receptor for glucagon-like peptide-I: brain, heart and pancreatic forms have the same deduced amino acid sequences. *FEBS Lett.* 358, 219–224. doi: 10.1016/0014-5793(94)01430-9
- Williams, E. K., Chang, R. B., Strohlic, D. E., Umans, B. D., Lowell, B. B., and Liberles, S. D. (2016). Sensory Neurons that Detect Stretch and Nutrients in the Digestive System. *Cell* 166, 209–221. doi: 10.1016/j.cell.2016.05.011
- Zhang, Y., Zheng, Y., Fu, Y., and Wang, C. (2019). Identification of biomarkers, pathways and potential therapeutic agents for white adipocyte insulin resistance using bioinformatics analysis. *Adipocyte* 8, 318–329. doi: 10.1080/21623945.2019.1649578